

Induced Violation of Time-Reversal Invariance in the Regime of Weakly Overlapping Resonances

B. Dietz,¹ T. Friedrich,^{1,2} H. L. Harney,³ M. Miski-Oglu,¹ A. Richter,^{1,4,*} F. Schäfer,¹
J. Verbaarschot,⁵ and H. A. Weidenmüller³

¹*Institut für Kernphysik, Technische Universität Darmstadt, D-64289 Darmstadt, Germany*

²*GSI Helmholtzzentrum für Schwerionenforschung GmbH, D-64291 Darmstadt, Germany*

³*Max-Planck-Institut für Kernphysik, D-69029 Heidelberg, Germany*

⁴*ECT*, Villa Tambosi, I-38100 Villazzano (Trento), Italy*

⁵*Department of Physics and Astronomy, SUNY at Stony Brook, New York 11794, USA*

(Received 21 January 2009; published 3 August 2009)

We measure the complex scattering amplitudes of a flat microwave cavity (a “chaotic billiard”). Time-reversal (\mathcal{T}) invariance is partially broken by a magnetized ferrite placed within the cavity. We extend the random-matrix approach to \mathcal{T} violation in scattering, determine the parameters from some properties of the scattering amplitudes, and successfully predict others. Our work constitutes the most precise test of the random-matrix theoretical approach to \mathcal{T} violation so far available.

DOI: 10.1103/PhysRevLett.103.064101

PACS numbers: 05.45.Mt, 11.30.Er, 24.60.Ky, 85.70.Ge

We measure the effect of partial violation of time-reversal (\mathcal{T}) invariance on the excitation functions of a flat microwave cavity induced by a magnetized ferrite placed within the cavity. The classical dynamics of a point particle moving freely within the cavity and elastically reflected by the walls is chaotic. The generic statistical properties of the eigenvalues and eigenfunctions of the analogous quantum system are, therefore, expected to follow random-matrix theory (RMT) predictions [1], which provide a universal description. In particular, RMT yields analytical expressions for correlation functions of scattering amplitudes [2] that can be generalized to include \mathcal{T} violation. Although widely used (to discover signatures of \mathcal{T} violation in compound-nucleus reactions [3] in the Ericson regime [4], to describe electron transport through mesoscopic samples in the presence of a magnetic field [5], and in ultrasound transmission in rotational flows [6]), we expose that generic model for \mathcal{T} violation, to the best of our knowledge, for the first time to a detailed experimental test.

Our aim is not a detailed dynamical modeling of the properties of the cavity. We determine the parameters of the RMT expressions from fits to some of the data. We then test the RMT approach by using it to predict other data, and by subjecting our fits to a thorough statistical test. All of this is in the spirit of a generic RMT approach since a dynamical calculation of the relevant parameters is possible only for certain chaotic quantum systems, if, e.g., the semiclassical approximation can be used [7]. We use that approximation only to determine the average level density, and to estimate the range of validity of RMT in terms of the shortest periodic orbit.

Microwave cavities have been used before to study the effect of \mathcal{T} violation on the eigenvalues [8,9] and on the eigenfunctions [10]. Here we study fluctuations of the scattering amplitudes versus microwave frequency in a regime, where the average resonance spacing d is smaller or of the order of the resonance width Γ .

Experiment.—The flat copper microwave resonator has the shape of a tilted stadium [11] (see Fig. 1) and a height of 5 mm. The frequency f ranges from 1 to 25 GHz, where only one vertical mode of the electric field strength is excited. The Helmholtz equation is then mathematically equivalent to the Schrödinger equation of the two-dimensional quantum billiard [12]. An Agilent PNA-L N5230A vector network analyzer (VNA) coupled rf energy via one of two antennas labeled 1 and 2 into the resonator and determined magnitude and phase of the transmitted (reflected) signal at the other (same) antenna in relation to the input signal and, thus, the elements $S_{ab}(f)$ with $a, b = 1, 2$ of the complex-valued 2×2 scattering matrix. Distorting effects of the connecting coaxial cables were removed by calibration. We measured the elements of $S(f)$ at a resolution of 100 kHz. To improve the statistical significance of the data set, an additional scatterer (an iron disc of 20 mm diameter) was placed within the cavity. It could be freely moved and allowed the measurement of statistically independent spectra, so-called “realizations.”

Time-reversal invariance is violated [13] by a ferrite cylinder ($4\pi M_S = 1859$ Oe, $\Delta H = 17.5$ Oe, courtesy of AFT Materials GmbH, Backnang, Germany) of 4 mm diameter and 5 mm height. The cylinder was placed inside the resonator and magnetized by an external magnetic field B of two NdFeB magnets from outside. Field strengths of up to 360 mT could be attained. Here we focus on the

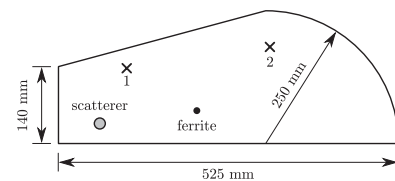


FIG. 1. The tilted-stadium billiard (schematic). The two antennas 1, 2 connect the resonator to the VNA. The ferrite is fixed, the scatterer can be moved freely.

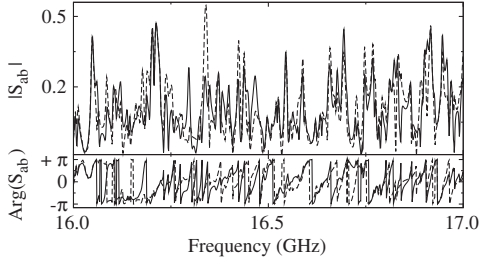


FIG. 2. Transmission spectra for $B = 190$ mT in the range 16–17 GHz. The amplitudes and phases of S_{12} (solid) and S_{21} (dashed) are seen to differ.

results at $B = 190$ mT as there the effects are most clearly visible. The spins within the ferrite precess collectively with their Larmor frequency about the external field. The rf magnetic fields of the resonator modes are, in general, elliptically polarized and couple to the spins of the ferrite. The coupling depends on the rotational direction of the rf field. An interchange of input and output channels changes the rotational direction and thus the coupling. Figure 2 demonstrates that reciprocity, defined by $S_{12}(f) = S_{21}(f)$ and implied by \mathcal{T} invariance, is violated. As a measure of the strength of \mathcal{T} violation, we define the cross-correlation coefficient $C_{\text{cross}}(\epsilon = 0)$ where

$$C_{\text{cross}}(\epsilon) = \frac{\text{Re}[\langle S_{12}(f)S_{21}^*(f + \epsilon) \rangle]}{\sqrt{\langle |S_{12}(f)|^2 \rangle \langle |S_{21}(f)|^2 \rangle}}. \quad (1)$$

If \mathcal{T} invariance holds, we have $C_{\text{cross}}(0) = 1$ while S_{12} and S_{21} are uncorrelated and thus $C_{\text{cross}}(0) = 0$ if it is completely broken. The average $\langle \cdot \rangle$ over the data is taken in frequency windows of width 1 GHz and over 6 realizations. The upper panel of Fig. 3 shows $C_{\text{cross}}(0)$ for the different frequency windows. It depends strongly on f although complete violation of \mathcal{T} is never attained. At 5–7 GHz the Larmor frequency of the ferrite matches the rf frequency, resulting in $C_{\text{cross}}(0) \approx 0.8$. Surprisingly, around 15 GHz the effects of \mathcal{T} violation are strongest, $C_{\text{cross}}(0) \approx 0.5$. A third minimum is observed at about 24 GHz.

Analysis.—We analyze the data with a scattering approach developed in the context of compound-nucleus reactions [14]. The matrix for the scattering from antenna b to antenna a is written as $S_{ab}(f) = \delta_{ab} - 2\pi i [W^\dagger(f - H^{\text{eff}})^{-1}W]_{ab}$. The matrix $W_{\mu a}$ is rectangular and describes the coupling of the N resonant states μ in the cavity with the antennas $a = 1, 2$. We assume that \mathcal{T} violation is due to the ferrite only. Then $W_{\mu a}$ is real. The resonances in the cavity are modeled by $H^{\text{eff}} = H - i\pi\tilde{W}\tilde{W}^\dagger$. Here H is the

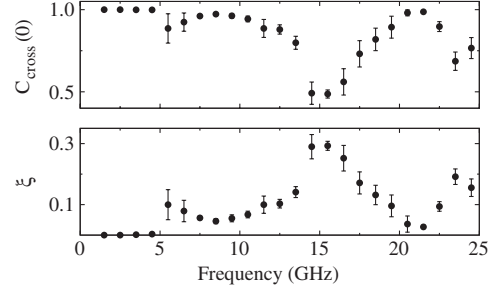


FIG. 3. Experimental values of $C_{\text{cross}}(0)$ (upper panel) from Eq. (1) and the parameter ξ for \mathcal{T} violation deduced from these (lower panel) with the help of Eq. (3). The error bars indicate the rms variation of $C_{\text{cross}}(0)$ over the 6 realizations.

Hamiltonian of the closed resonator. The elements of the real matrix $\tilde{W}_{\mu c}$ are equal to those of $W_{\mu c}$ for $c = 1, 2$. As done successfully before [15,16], Ohmic absorption of the microwaves in the walls of the cavity and the ferrite is mimicked [17] by additional fictitious weakly coupled channels c . As the billiard dynamics is chaotic [1], we model H by an ensemble of N -dimensional random matrices, which are written as the sum of two parts [18,19], $H = H^s + i(\pi\xi/\sqrt{N})H^a$. The real, symmetric, and \mathcal{T} invariant matrix H^s is taken from the Gaussian orthogonal ensemble (GOE) while the real, antisymmetric matrix H^a with Gaussian-distributed matrix elements models the \mathcal{T} breaking part of H . For $\pi\xi/\sqrt{N} = 1$ the Hamiltonian H belongs to the Gaussian unitary ensemble (GUE) systems with complete \mathcal{T} breaking. However, for $N \rightarrow \infty$, \mathcal{T} invariance is significantly broken already when the dimensionless parameter ξ is close to unity [20]. In the same limit $C_{\text{cross}}(0)$ in Eq. (1) can be expressed in terms of a threefold integral involving ξ . For the derivation we extended the method of Ref. [21] where the ensemble average of $|S_{ab}|^2$ was computed as function of ξ . With the notations

$$\begin{aligned} t &= \pi^2 \xi^2, & \mathcal{R} &= 4(x + x_1)(x + x_2), \\ \mathcal{U} &= 2\sqrt{x_1(1 + x_1)x_2(1 + x_2)}, \\ \mathcal{F} &= 4x(1 - x), & \mathcal{E}_\pm &= 1 \pm \exp(-2t\mathcal{F}), & \lambda &= 1 - 2x, \\ \lambda_i &= \sqrt{(1 + x_1)(1 + x_2) + x_1x_2 - (-1)^i \mathcal{U}}, \\ \mathcal{G}_i &= \lambda_i^2 - 1, & i &= 1, 2 \end{aligned} \quad (2)$$

the cross-correlation coefficient $C_{\text{cross}}(0)$ is obtained by setting $\epsilon = 0$, $\sigma = -1$, and $a, b = 1, 2$ in the function

$$\begin{aligned} F_{ab}^\sigma(\epsilon|T_a, T_b, \tau_{\text{abs}}, \xi) &= \frac{1}{8} \int_0^\infty dx_1 \int_0^\infty dx_2 \int_0^1 dx \frac{\mu(x, x_1, x_2)}{\mathcal{F}} \exp\left[-\frac{i\pi\epsilon}{d}(x_1 + x_2 + 2x)\right] \prod_c \frac{1 - T_c x}{\sqrt{(1 + T_c x_1)(1 + T_c x_2)}} \\ &\times \left[J_{ab}(x, x_1, x_2) [\mathcal{F}\mathcal{E}_+ + (\lambda_2^2 - \lambda_1^2)\mathcal{E}_- + 4t\mathcal{R}(\lambda_2^2\mathcal{E}_- + \mathcal{F}(\mathcal{E}_+ - 1))] + \sigma 2(1 - \delta_{ab})T_a T_b \right. \\ &\times \left. \left[\mathcal{E}_- K_{ab}(\lambda, \lambda_1, \lambda_2|T_a, T_b, \xi) + \left(\mathcal{E}_+ - \frac{\mathcal{E}_-}{t\mathcal{F}}\right) L_{ab}(\lambda, \lambda_1, \lambda_2|T_a, T_b, \xi) \right] \right] \exp(-2t\mathcal{G}_2) + (\lambda_1 \leftrightarrow \lambda_2). \end{aligned} \quad (3)$$

The integration measure $\mu(x, x_1, x_2)$ and the function $J_{ab}(x, x_1, x_2)$ are given in Ref. [2], while the functions $K_{ab}(\lambda, \lambda_1, \lambda_2|T_a, T_b, \xi)$ and $L_{ab}(\lambda, \lambda_1, \lambda_2|T_a, T_b, \xi)$ can be read off Eq. (2) of Ref. [22]. We checked our analytic results by numerical RMT simulations. The parameters of Eq. (3) are d, ξ , the transmission coefficients $T_a = 1 - |S_{aa}|^2$ for $a = 1, 2$, and the sum τ_{abs} of 300 transmission coefficients that model the Ohmic losses [16,17].

For a typical set $T_1, T_2, \tau_{\text{abs}}$, Fig. 4 shows $C_{\text{cross}}(0)$ versus ξ . Within the frequency range 1–25 GHz, $C_{\text{cross}}(0)$ depends very weakly on $T_1, T_2, \tau_{\text{abs}}$, and Fig. 4 can be taken to be universal. For each data point shown in the upper panel of Fig. 3 the corresponding value of ξ was read off Fig. 4 and the result is shown in the lower panel of Fig. 3. The strength ξ of \mathcal{T} breaking varies from zero to 0.3. Numerical calculations show that for $\xi = 0.3$ the spectral fluctuations of the Hamiltonian H almost coincide with those of the GUE [23]. We also found that for $\xi = 0.4$ they do not differ significantly from those presented in Ref. [8], where the conclusion was drawn, that complete \mathcal{T} breaking is achieved, whereas the value of $C_{\text{cross}}(0)$ is still far from zero. This shows that $C_{\text{cross}}(0)$ is a particularly suitable measure of the strength ξ of \mathcal{T} violation.

Autocorrelation function.—Since $C_{\text{cross}}(0)$ depends only weakly on T_1, T_2 , and τ_{abs} , we used the autocorrelation function $C_{ab}(\epsilon)$ for their more precise determination, especially of τ_{abs} . The function

$$C_{ab}(\epsilon) = \langle S_{ab}(f)S_{ab}^*(f + \epsilon) \rangle - |\langle S_{ab}(f) \rangle|^2 \quad (4)$$

was calculated with the method of Ref. [21] as a function of $T_1, T_2, \tau_{\text{abs}}, \xi$, and d and is obtained from Eq. (3) by setting $\sigma = +1$. It interpolates between the well-known results for orthogonal symmetry [2] (full \mathcal{T} invariance) and for unitary symmetry [24] (complete violation of \mathcal{T} invariance). The mean level spacing d was computed from the Weyl formula. The Fourier transform of $C_{ab}(\epsilon)$ was then fitted to the data as in Ref. [16]. As starting points we used the values of T_1 and T_2 from the measured values of $S_{aa}(f)$ and of ξ determined from $C_{\text{cross}}(0)$. For each of the 6 realizations the spectra of $S_{ab}(f)$ were divided into intervals Δf of 1 GHz length. In each interval the Fourier transform $\tilde{C}_{ab}(t_k)$ of the autocorrelation function

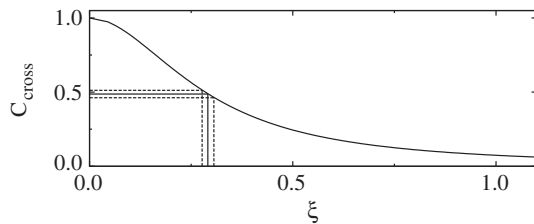


FIG. 4. Dependence of the cross-correlation coefficient $C_{\text{cross}}(0)$ on the parameter ξ as predicted by the random-matrix model for partial violation of \mathcal{T} invariance. Also shown is how $C_{\text{cross}}(0) = 0.49(3)$ translates into $\xi = 0.29(2)$.

(4) was calculated for values of t_k between 5 and 200 ns. The lower limit is determined by the length of the shortest periodic orbit in the classical billiard [7]; for smaller values of t_k the Fourier coefficients are nongeneric. At $t_k \approx 200$ ns the values of $\tilde{C}_{ab}(t_k)$ have decayed over more than 3 orders of magnitude, and noise limits the analysis. The time resolution was $1/\Delta f = 1$ ns. We measured the four excitation functions $S_{ab}(f)$ taking $a, b = 1, 2$ yielding a total of 4800 Fourier coefficients for each interval. For $f > 10$ GHz the fitted values for T_1 and T_2 differ by not more than 7% from the initial ones. For smaller f the intervals of 1 GHz width comprise only few resonances. The spread of the data is large, see the left panel of Fig. 5. Going to the time domain is useful since the $S_{ab}(f)$ are correlated for neighboring f whereas the correlations are removed in the ratios of the experimental and the fitted values for $\tilde{C}_{ab}(t_k)$. The latter are stationary and fluctuate about unity. For each realization the parameters τ_{abs} and ξ were obtained by fitting the analytical expression for $\tilde{C}_{ab}(t_k)$ to the experimental results. The values of ξ determined from these fits agree with the ones found from the cross-correlation coefficient. To reduce the spread we combined the data from all realizations within a fixed frequency interval. The result was analyzed with a goodness-of-fit (GOF) test (see Ref. [16]) that distinguishes between full, partial, and no violation of \mathcal{T} . We defined a confidence limit such that the GOF test erroneously rejects a valid theoretical description of the data with a probability of 10%. With this confidence limit the test rejects the fitted expressions for $\tilde{C}_{ab}(t_k)$ in only 1 out of the 24 available frequency windows or in 4.2% of the tests. The ratio of the average resonance width Γ to the average resonance spacing d varies from $\Gamma/d \approx 0.01$ to $\Gamma/d \approx 1.2$. Thus, the RMT model correctly describes the fluctuations of the S -matrix for partial \mathcal{T} violation in the regimes of isolated and weakly overlapping resonances.

Elastic enhancement factor.—As a second test of the theory we use the determined values of $\xi, T_a, T_b, \tau_{\text{abs}}$ to predict the elastic enhancement factor \mathcal{W} as a

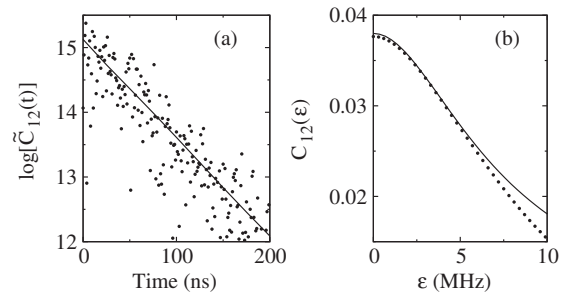


FIG. 5. Autocorrelation function for S_{12} in the range of 16–17 GHz and at $B = 190$ mT. In the time domain (a) the data (dots) scatter around the theoretical fit (solid) for $T_1 = 0.37, T_2 = 0.41, \tau_{\text{abs}} = 2.9$ and $\xi = 0.25$. Transforming the results back into frequency domain (b) confirms the good agreement between data and theory. We observe that neighboring data points in (b) are correlated, whereas those in (a) are not.

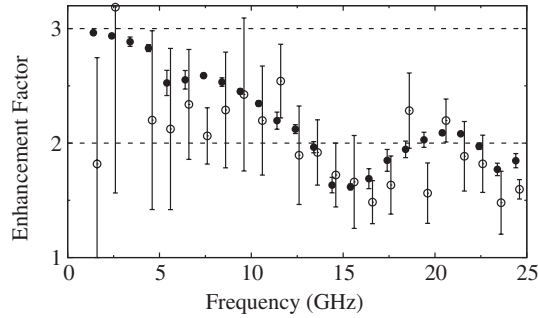


FIG. 6. Elastic enhancement factors \mathcal{W} determined from the data (open circles) and from the analytic result for partial \mathcal{T} violation (filled circles) using the fitted parameters. The error bars indicate the variations within the 6 realizations. The dashed horizontal lines indicate the limits of \mathcal{W} for \mathcal{T} invariant systems.

function of f , which with Eq. (4) is given as $\mathcal{W} = \sqrt{C_{11}(0)C_{22}(0)}/C_{12}(0)$. For \mathcal{T} invariant systems, \mathcal{W} decreases from 3 for isolated resonances with many weakly coupled open channels to 2 for strongly overlapping resonances ($\Gamma \gg d$). The corresponding values for complete \mathcal{T} violation are $\mathcal{W} = 2$ and $\mathcal{W} = 1$, respectively [25]. Figure 6 compares the analytic results for \mathcal{W} (filled circles) to the data (open circles). For small f (where $\Gamma/d \ll 1$ and $\xi \approx 0$) the experimental results differ from the prediction $\mathcal{W} = 3$. Here only few resonances contribute and the errors of the experimental values for \mathcal{W} are large. Moreover \mathcal{W} is determined from only a single value $C_{ab}(0)$ of the measured autocorrelation function while the analytic result is based on a fit of the complete autocorrelation function. As f increases so does Γ/d , and \mathcal{W} takes values well below 3. At frequencies where ξ is largest \mathcal{W} drops below 2, a situation that cannot arise for \mathcal{T} invariant systems. The overall agreement between both data sets above ≈ 10 GHz corroborates the confidence in the values of ξ deduced from $C_{\text{cross}}(0)$.

Summary.—We have investigated partial violation of \mathcal{T} invariance with the help of a magnetized ferrite placed inside a chaotic microwave billiard. We measured reflection and transmission amplitudes in the regime of isolated and weakly overlapping resonances and determined the cross-correlation function, the autocorrelation functions, and the elastic enhancement factor from the data. The results were used as a test of RMT for scattering processes with partial \mathcal{T} violation which yields analytic expressions for all three observables. The parameters of the theory (T_1 , T_2 , τ_{abs} and the parameter ξ for \mathcal{T} violation) were partly obtained directly from the data but improved values resulted from fits to the autocorrelation function. The validity of the theory was tested in two ways. (i) A goodness-of-fit test of the Fourier coefficients of the scattering matrix yielded excellent agreement. (ii) The elastic enhancement

factor predicted from the fitted values of the parameters shows overall agreement with the data. We conclude that the random-matrix description of S -matrix fluctuations with partially broken \mathcal{T} invariance is in excellent agreement with the data.

F.S. is grateful for the financial support from the Deutsche Telekom Foundation. This work was supported by the DFG within SFB 634.

*richter@ikp.tu-darmstadt.de

- [1] O. Bohigas, M.J. Giannoni, and C. Schmit, *Phys. Rev. Lett.* **52**, 1 (1984).
- [2] J.J.M. Verbaarschot, H.A. Weidenmüller, and M.R. Zirnbauer, *Phys. Rep.* **129**, 367 (1985).
- [3] W. von Witsch, A. Richter, and P. von Brentano, *Phys. Rev. Lett.* **19**, 524 (1967); E. Blanke *et al.*, *ibid.* **51**, 355 (1983).
- [4] T. Ericson, *Phys. Rev. Lett.* **5**, 430 (1960).
- [5] G. Bergman, *Phys. Rep.* **107**, 1 (1984).
- [6] J. Rosny *et al.*, *Phys. Rev. Lett.* **95**, 074301 (2005).
- [7] R. Blümel and U. Smilansky, *Phys. Rev. Lett.* **64**, 241 (1990); **60**, 477 (1988).
- [8] P. So *et al.*, *Phys. Rev. Lett.* **74**, 2662 (1995).
- [9] U. Stoffregen *et al.*, *Phys. Rev. Lett.* **74**, 2666 (1995); O. Hul *et al.*, *Phys. Rev. E* **69**, 056205 (2004).
- [10] D.H. Wu *et al.*, *Phys. Rev. Lett.* **81**, 2890 (1998).
- [11] H. Primack and U. Smilansky, *J. Phys. A* **27**, 4439 (1994).
- [12] H.-J. Stöckmann and J. Stein, *Phys. Rev. Lett.* **64**, 2215 (1990).
- [13] B. Dietz *et al.*, *Phys. Rev. Lett.* **98**, 074103 (2007).
- [14] C. Mahaux and H.A. Weidenmüller, *Shell-Model Approach to Nuclear Reactions* (North-Holland Publ. Co., Amsterdam, 1969).
- [15] C.H. Lewenkopf and A. Müller, *Phys. Rev. A* **45**, 2635 (1992); R. Schäfer *et al.*, *J. Phys. A* **36**, 3289 (2003).
- [16] B. Dietz *et al.*, *Phys. Rev. E* **78**, 055204(R) (2008).
- [17] P.W. Brouwer and C.W.J. Beenakker, *Phys. Rev. B* **55**, 4695 (1997).
- [18] A. Pandey, *Ann. Phys. (N.Y.)* **134**, 110 (1981); A. Pandey and M.L. Mehta, *Commun. Math. Phys.* **87**, 449 (1983).
- [19] A. Altland, S. Iida, and K.B. Efetov, *J. Phys. A* **26**, 3545 (1993).
- [20] Time-reversal invariance is significantly broken for $\pi\xi/\sqrt{N} \approx d/v$. Here, $d = v\pi/\sqrt{N}$ denotes the average level spacing and v^2 the variance of the off-diagonal matrix elements of H^s, H^a .
- [21] Z. Pluhař *et al.*, *Ann. Phys. (Leipzig)* **243**, 1 (1995).
- [22] U. Gerland and H.A. Weidenmüller, *Europhys. Lett.* **35**, 701 (1996).
- [23] O. Bohigas *et al.*, *Nonlinearity* **8**, 203 (1995).
- [24] Y.V. Fyodorov, D.V. Savin, and H.-J. Sommers, *J. Phys. A* **38**, 10731 (2005).
- [25] D.V. Savin, Y.V. Fyodorov, and H.-J. Sommers, *Acta Phys. Pol. A* **109**, 53 (2006).